Bioactive Materials 15 (2022) 131–144

Contents lists available at ScienceDirect

Bioactive Materials

journal homepage: www.keaipublishing.com/en/journals/bioactive-materials

Turning gray selenium into a nanoaccelerator of tissue regeneration by PEG modification

Jieqiong Cao [a,1], Yibo Zhang [a,1], Peiguang Zhang [a], Zilei Zhang [a], Bihui Zhang [a], Yanxian Feng [d], Zhixin Li [a], Yiqi Yang [a], Qilin Meng [a], Liu He [a], Yulin Cai [a], Zhenyu Wang [a], Jie Li [a], Xue Chen [a], Hongwei Liu [c], An Hong [a,**], Wenjie Zheng [b,***], Xiaojia Chen [a,e,*]

[a] Institute of Biomedicine & Department of Cell Biology, College of Life Science and Technology, Jinan University, Guangdong Province Key Laboratory of Bioengineering Medicine, Guangdong Provincial biotechnology drug & Engineering Technology Research Center, National Engineering Research Center of Genetic Medicine, Guangzhou, China

[b] Department of Chemistry, Jinan University, Guangzhou, China

[c] Department of Plastic Surgery, The First Affiliated Hospital of Jinan University, Guangzhou, 510630, China

[d] School of Biotechnology and Health Sciences, Wuyi University, Jiangmen, 529020, China

[e] Guangzhou Red Cross Hospital, Jinan University, Guangzhou 510240, China

ARTICLE INFO

Keywords:
PEG modification
Nanoselenium
Tissue regeneration
Zebrafish

ABSTRACT

Selenium (Se) is an essential trace element involved in nearly all human physiological processes but suffers from a narrow margin between benefit and toxicity. The nanoform of selenium has been proven shown to be more bioavailable and less toxic, yet significant challenges remain regarding the efficient and feasible synthesis of biologically active nanoselenium. In addition, although nanoselenium has shown a variety of biological activities, more interesting nanoselenium features are expected. In this work, hydrosoluble nanoselenium termed Nano-Se in the zero oxidation state was synthesized between gray Se and PEG. A zebrafish screen was carried out in zebrafish larvae cocultured with Nano-Se. Excitingly, Nano-Se promoted the action of the FGFR, Wnt, and VEGF signaling pathways, which play crucial roles in tissue regeneration. As expected, Nano-Se not only achieved the regeneration of zebrafish tail fins and mouse skin but also promoted the repair of skin in diabetic mice while maintaining a profitable safe profile. In brief, the Nano-Se reported here provided an efficient and feasible method for bioactive nanoselenium synthesis and not only expanded the application of nanoselenium to regenerative medicine but also likely reinvigorated efforts for discovering more peculiarunique biofunctions of nanoselenium in a great variety of human diseases.

1. Introduction

Emerging nanomedicine holds great promise for new treatments because of its novel characteristic properties that are strikingly different from those of both isolated atoms and bulk material [1,2]. Selenium, of course, has proven to be one of the biggest beneficiaries of nanotechnology [3]. Compared with inorganic and organic forms, the nanoform of selenium is growingly yielding up the optimal bioavailability and lowered toxicity [4,5]. Both advantages of nanoselenium owes a good deal to the possibility of using selenium in the zero oxidation state (Se (0)), which favors the antioxidant bioactivity of Se and minimizes its chemical activity, which is the archcriminal toxicity [3,6]. According to relevant standards, the intake of selenium for persons over 18 years old is 50–250 μg/d [7]. Inappropriate intake of selenium can cause adverse

Peer review under responsibility of KeAi Communications Co., Ltd.

* Corresponding author. Institute of Biomedicine & Department of Cell Biology, College of Life Science and Technology, Jinan University, Guangdong Province Key Laboratory of Bioengineering Medicine, Guangdong Provincial biotechnology drug & Engineering Technology Research Center, National Engineering Research Center of Genetic Medicine, Guangzhou, China.

** Corresponding author.

*** Corresponding author.

E-mail addresses: tha@jnu.edu.cn (A. Hong), tzhwj@jnu.edu.cn (W. Zheng), tchenxj@jnu.edu.cn (X. Chen).

[1] These authors contributed equally to this work.

https://doi.org/10.1016/j.bioactmat.2021.12.026
Received 7 July 2021; Received in revised form 30 November 2021; Accepted 21 December 2021
Available online 2 January 2022

reactions. Excessive intake of selenium could cause skin pain dullness, numbness of limbs, dizziness, gastrointestinal disorders, and indigestion. Moreover, selenium deficiency can also lead to cardiomyopathy, myocardial failure, and Keshan disease and so on [8]. However, using Se (0) is both a blessing and a curse: its poor solubility in physiological buffer severely limits its application. Thus, the construction of dissolvable nanoselenium has always been a challenge.

To overcome this, three general strategies have emerged for water-soluble nanoselenium synthesis: 1) employing physical methods such as microwave irradiation [9], ultraviolet irradiation [10], laser ablation [11], and ultrasonic field treatment [12]; 2) using chemical reagents including but not limited to $NaBH_4$ [13], ascorbic acid [14,15], BSA [16] and citric acid [17] to reduce some acids containing selenium; and 3) borrowing biological identities, for example, microorganisms [18] cells and plants [19], to synthesize dissolvable nanoselenium. Nevertheless, the first physical method always suffers from a resource-intensive and laborious process [20]. Although the second chemical method is time-saving, it harms the environment because of harmful chemicals [21]. Third eco-friendly biological methods have received more attention in comparison to both fronts, but the uncontrollable synthesis process and the synthesis products limit their extensive application [22]. While some success has been achieved in synthesizing dissolvable nanoselenium using these three strategies, significant challenges remain regarding the efficient and feasible synthesis of biologically active nanoselenium. Toward this end, a one-pot strategy was developed to gray Se with polyethylene glycol (PEG) at 200–220 °C, resulting in a hydrosoluble nanoselenium (termed Nano-Se) in the zero oxidation state.

In terms of biological activities, selenium has can affect many physiological processes, including but not limited to growth, development, immunomodulation, and reproduction [23], thereby having widespread applications as bioantioxidants [24], antibiotics [25], antineoplastic agents [26], antidiabetic agents [27], and nutritional supplements [28]. Owing to its optimal bioavailability and lower toxicity in comparison to inorganic and organic forms, the nanoform of selenium is preferred for therapy for diseases such as cancer, muscular dystrophy, diabetes, liver fibrosis, and infection [29]. While nanoselenium has been regarded as an excellent alternative to inorganic and organic selenium, more distinctive nanoselenium features are expected. To this end, many *in vitro* cultured cells have been used to screen new functions of nanoparticles, which limits the screening of cell-autonomous phenotypes. Although some *in vivo* models established in different mice with various diseases can overcome this limitation, screens carried out in mouse models always require a mass of nanoparticles and possess extremely limited throughput [30]. To overcome functional limitations in cells and throughput limitations in mice, emerging zebrafish have become a prominent vertebrate model for drug and functional material discovery [31]. With a high-quality zebrafish genome that is 71% orthologous to human beings [32], zebrafish exhibit a diverse repertoire of human biological processes and possess fully integrated vertebrate organ systems like human beings [31]. As in the following, a broader range of accessible biology can be assayed in zebrafish in comparison with cultured cells, and a higher throughput can be achieved in contrast to mouse models.

Herein, hydrosoluble Nano-Se in the zero oxidation state was synthesized between gray Se and PEG. A zebrafish screen was carried out in zebrafish larvae cocultured with Nano-Se. Excitingly, Nano-Se promoted the action of the FGFR, Wnt and VEGF signaling pathways, which play crucial roles in tissue regeneration. This means that Nano-Se has great potential to be a safe and degradable nanoaccelerator of regeneration. To test this hypothesis, a zebrafish tail fin regeneration model and a mouse skin regeneration model were used to challenge the regeneration promotion capacity of Nano-Se. As expected, Nano-Se not only achieved the regeneration of zebrafish tail fins and mouse skin but also promoted the repair of skin in diabetic mice while maintaining a profitable safe profile. In brief, the nano-Se reported here provided an efficient and feasible method for bioactive nanoselenium synthesis and expanded the application of nanoselenium to regenerative medicine.

2. Results

2.1. Synthesis and characterization of Nano-Se

As the first step toward this study, Nano-Se was synthesized by heating gray Se to 200–220 °C in polyethylene glycol (PEG) for 30 min, followed by hydration with cold Milli-Q water (Fig. 1A). Dynamic light scattering (DLS) (Fig. 1B) was measured in the Nano-Se solution, which demonstrated an average diameter of approximately 144 nm. Typical transmission electron microscopy (Fig. 1C), high resolution transmission electron microscope (Fig. S1A) and atomic force microscopy (Fig. 1D) images showed that Nano-Se is a spherical structure with a diameter of approximately 100–150 nm (Fig. 1C and D), which is consistent with the DLS result and stable in aqueous solution and DMEM (10% FBS) for 14 days (Fig. S2). The Se concentration of the Nano-Se solution was quantified by employing ICP (Table S1) and EDS analysis (Fig. S1B).

2.2. Nano-Se promotes the tissue regeneration

Recently, zebrafish, a nonmammalian vertebrate, has become one of the top disease models for investigation because the similarity of its genome reaches as high as 70% with that of humans [33]. It can regenerate its heart [34,35], retina [36], kidney [37,38], liver [39,40], and appendants, for instance, the fins [41–43], throughout its entire life, which makes zebrafish one of the most popular models for studying tissue regeneration. Among regenerable organs, the tail fin, which is well organized with vessels, nerves, and stromal structures and comprises skin, mesenchyme, and bone frames, has become a popular model for studying tissue regeneration due to its repeatability, ease of manipulation, and timesaving [44]. Therefore, the zebrafish tail fin model was selected first to investigate the regeneration-enhancing activities of nano-Se in this study. We performed caudal fin amputation on adult zebrafish, followed by exposure to Nano-Se. The resection rate and regeneration rate of zebrafish fin were calculated according to the formula demonstrated in Fig. 2A, and the resection rate in all groups remained similar (Fig. S4). As shown in Fig. 2B, the regeneration of zebrafish caudal fins was dramatically improved after 6 and 9 days of treatment with Nano-Se (100 nM). Quantification results demonstrated that the amputated zebrafish caudal fin with 4-day exposure to Nano-Se achieved a regeneration rate of 12.67% compared to that of 9.48% in the control group; this difference continued growing, and until 8-day Nano-Se exposure, the regeneration rate reached 31.74%, while the control group showed only 25.08% (Fig. 2C).

To explore which pathway genes can be regulated by Nano-Se, transcriptome analysis was performed. Significant differences in transcriptome characteristics between the Nano-Se and control groups were indicated by using principal component analysis (PCA) (Fig. 1E). Moreover, the heatmap analysis demonstrated that 400 genes were upregulated, while 40 genes were downregulated after treatment with Nano-Se (Fig. 1F). KEGG pathway analysis indicated that the WNT and VEGF signaling pathways contributed to the enrichment of these upregulated genes (Fig. 1G). For instance, *fzd9a*, *rhocb*, *crebbpb* (WNT pathway), *mapk14a*, *pik3r3b*, and *pla2g4f.2* (VEGF pathway) were significantly upregulated (Fig. 1H). Interestingly, *fgfr1bl*, a member of the FGF pathway, was also upregulated (Fig. 1H). In addition, the expression of two selenoproteins (Selenol and Selenop) was elevated after exposure to Nano-Se, which further strengthened the local effect at the genetic level. These results indicate that Nano-Se could upregulate gene expression related to the FGF, VEGF, and WNT signaling pathways, suggesting that Nano-Se is involved in regulating angiogenesis, cell migration, and tissue regeneration.

Moreover, to study whether this regeneration enhancement activity is an excluding property of Nano-Se, we evaluated the effect of PEG200,

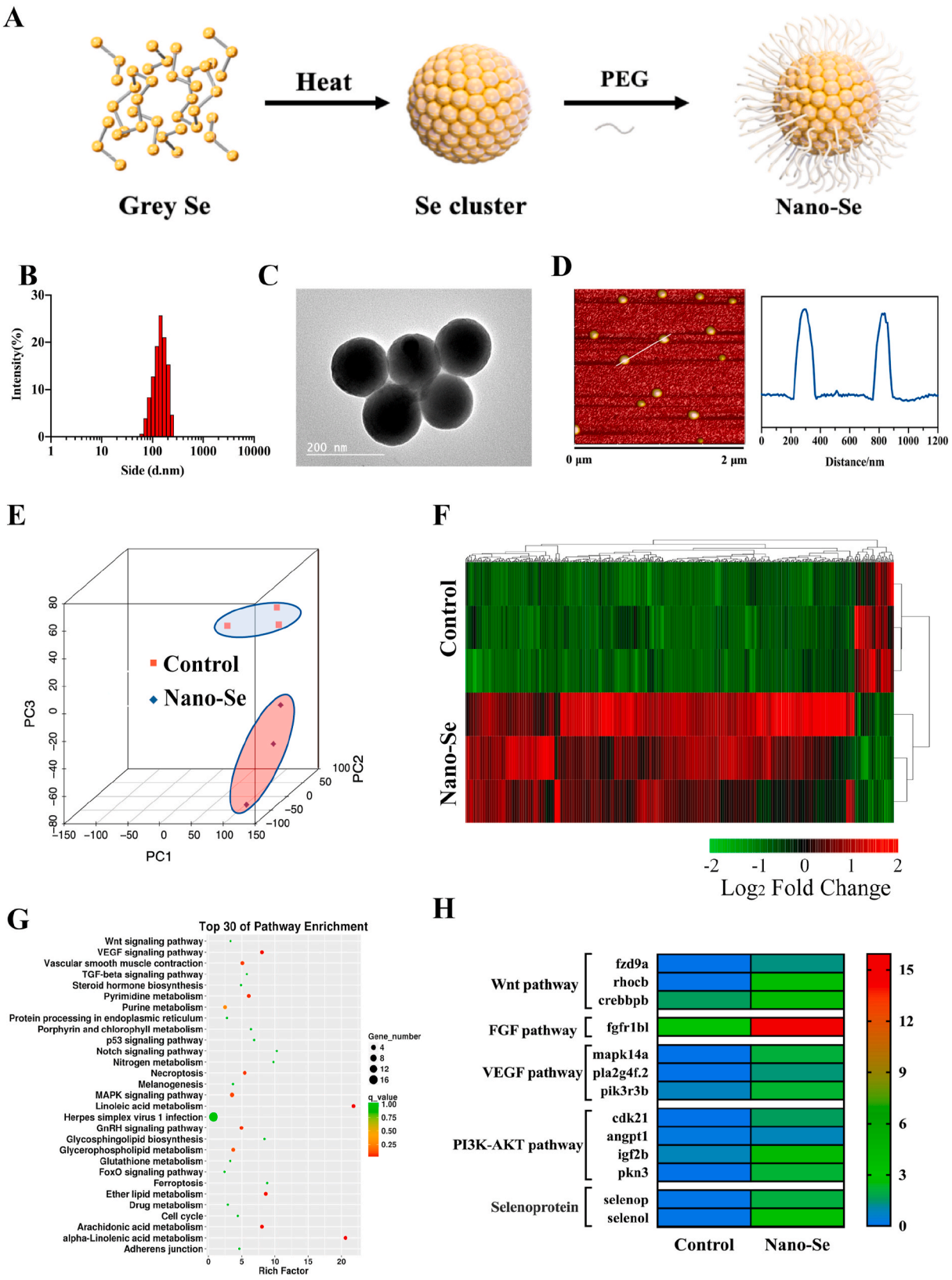

Fig. 1. **(A)** Schematic illustration synthesis of Nano-Se. **(B)** Particle size distribution of the Nano-Se. **(C)** TEM image of Nano-Se. Scale bars: 200 nm. **(D)** Atomic Force Microscope (AFM) image and particle size data analysis of Nano-Se. **(E)** Principal component analysis (PCA) was performed based on differentially expressed genes from regenerated tail fin the of two groups. Each data point corresponds to the PCA analysis of each sample. **(F)** Heat maps of significantly upregulated and downregulated genes (fold change ≥2 and $P < 0.05$). **(G)** KEGG pathway enrichment analysis of the identified differentially expressed genes. The 30 most significantly enriched pathways are shown. **(H)** Heat maps of significantly upregulated genes related to FGF, VEGF, Wnt pathway and selenoprotein.

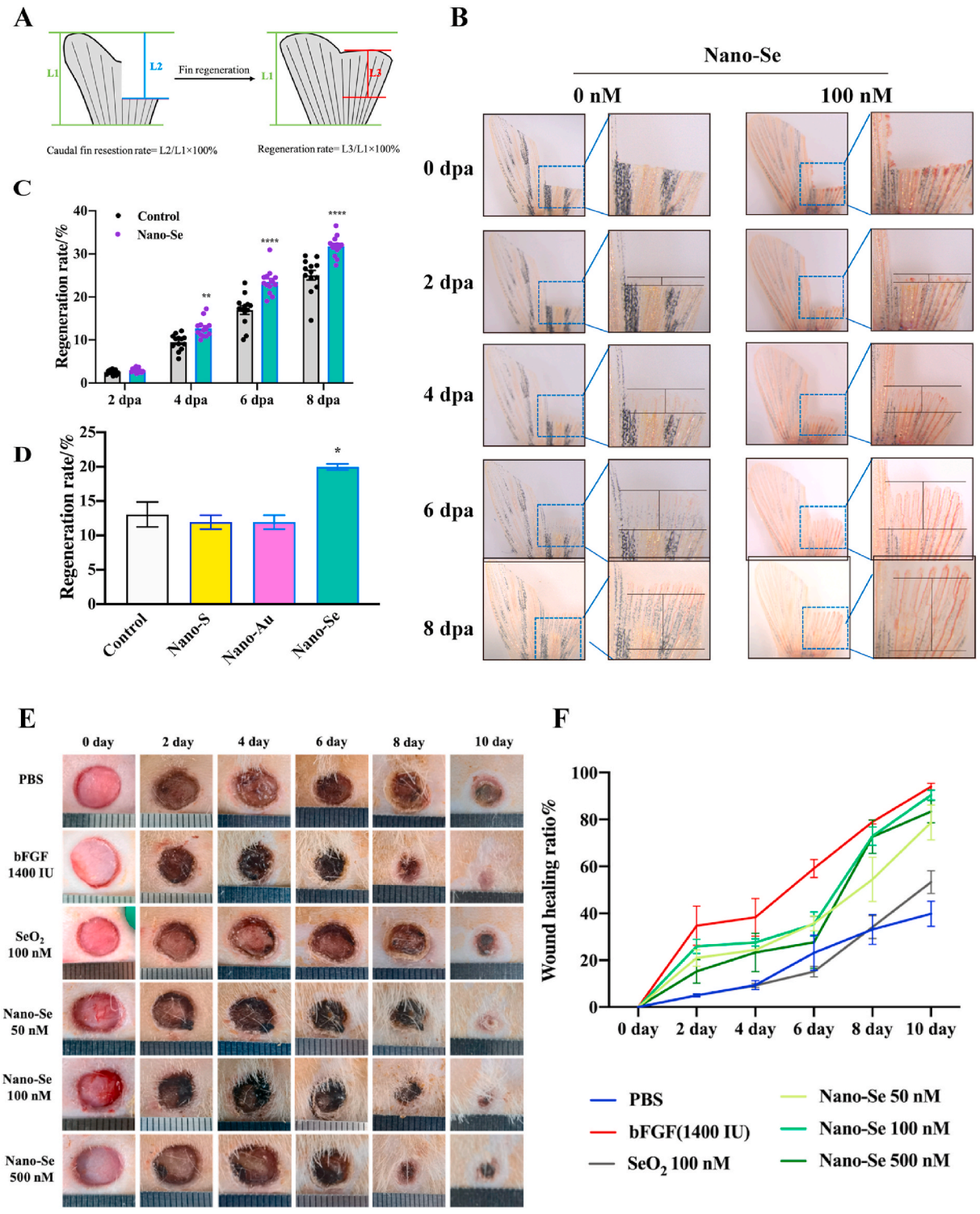

Fig. 2. **(A)** Schematic illustration of calculating the regeneration rate of zebrafish caudal fin. **(B)** Representative images of the Nano-Se accelerates caudal fin regeneration. dpa: days past amputation. **(C)** Regeneration rate of zebrafish caudal fin treated with Nano-Se. (3 independent biological repeats with a total n = 29). **(D)** Regeneration rate of adult zebrafish caudal fin treated with Nano-S, Nano-Au, Nano-Se (3 independent biological repeats with a total n = 15). **(E)** Representative images of Nano-Se in a dorsal cortex injury SD rats model. **(F)** Wound healing rate of Nano-Se in a dorsal cortex injury SD rats model (3 independent biological repeats with a total n = 15). (Mean values ± SD, *P < 0.05, **P < 0.01, ***P < 0.001, ****P < 0.0001).

selenite, Nano-S, and Nano-Au of similar sizes; however, the results demonstrated that neither Nano-S nor Nano-Au promoted the regeneration of zebrafish caudal fins (Fig. 2D, Figs. S5–6), and the same result was observed for selenite (Fig. S7) and PEG200 (Fig. S8). To study whether Nano-Se enhanced caudal fin regeneration in a local or distal manner, 6-coumarin was loaded in Nano-Se during synthesis, and the results indicated that 6-coumarin was distributed in the regenerated tail fin (Fig. S9). These results collectively indicate the unique regeneration enhancement activity of Nano-Se in a local manner.

The effect of Nano-Se on tissue regeneration was also verified in

mammalian SD rats. As shown in Fig. 2E, the skin wound healing rate was significantly accelerated. Quantification results demonstrated that the wound healing rate with 4-day exposure to Nano-Se achieved a regeneration rate of 27.51% compared to that of 9.36% in the control group; this difference continued growing, and until 10-day Nano-Se exposure, the regeneration rate reached 90.34%, while the control group showed only 39.78% (Fig. 2F).

2.3. Nano-Se promotes angiogenesis through the VEGF pathway

To investigate the importance of blood vessels in Nano-Se-induced zebrafish fin regeneration, a double transgenic zebrafish (fli1: EGFP/gata1: mCherry), in which endothelial cells and red blood cells are labeled with a green and red fluorescent protein, was employed to assess the impact of Nano-Se on blood vessel regeneration. The caudal fin of adult transgenic zebrafish was amputated to evaluate the effect of Nano-Se on blood vessels during fin regeneration. As shown in Fig. 3A and B, angiogenesis was elevated to 45.29% after treatment with Nano-Se (100 nM) for 6 days compared to 35.96% in the control group. Another zebrafish angiogenesis model, the subintestinal vein (SIVs), was also employed, and 24-h postfertilization (hpf) zebrafish embryos were incubated with 50 nM, 100 nM, and 200 nM Nano-Se for 48 h. The number of SIVs was also significantly increased after treatment with Nano-Se (100 nM) (Fig. S10). Moreover, we found that the number of branches of blood vessels increased significantly after Nano-Se treatment in the chicken embryo allantoic membrane experiment (Fig. 3C), indicating the stimulating effect of Nano-Se on angiogenesis.

To investigate whether the angiogenesis-enhancing activities of

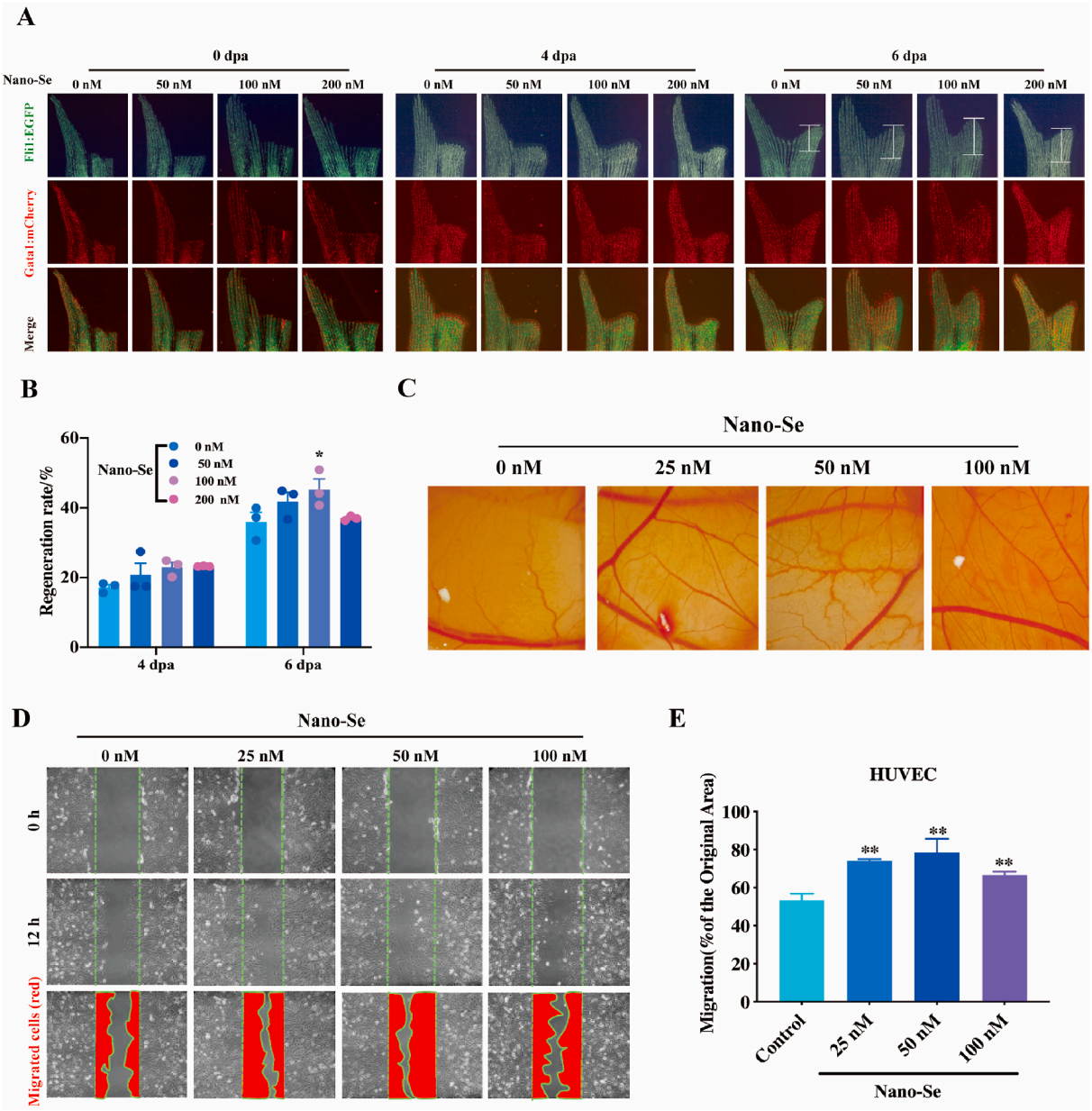

Fig. 3. **(A)** Representative fluorescence microscopy images for angiogenesis in fin regeneration by transgenosis zebrafish (*fli1*:EGFP/*gata1*:mCherry) which blood vessels were labeled with green fluorescence and blood with red fluorescence, the adult zebrafish were treated with different concentrations of Nano-Se (0, 50, 100 and 200 nM). **(B)** Regeneration rate of fin angiogenesis treated with Nano-Se (3 independent biological repeats with a total n = 13). **(C)** Nano-Se promotes angiogenesis of allantoic membrane of chicken embryo. **(D)** Wound healing assay to evaluate the migration of HUVEC cells after being treated with Nano-Se (0, 25, 50 and 100 nM) and DMEM with 10% FBS. Cells were wounded and monitored using a microscope 12 h. The red areas represent migrating cells. **(E)** Migration rate of HUVEC cells induced by Nano-Se (3 independent biological repeats with a total n = 9). (Mean values ± SD, *P < 0.05, **P < 0.01, ***P < 0.001, ****P < 0.0001).

Nano-Se are conserved in mammals, human umbilical vein endothelial cells (HUVECs) were employed for further investigation. After treatment with Nano-Se for 48 h, the number of EdU^+ cells, which represents cell division and proliferation, was significantly increased (Fig. S11) while the LD50 of Nano-Se was 523.4 nM (Fig. S13A) . Moreover, the migration of HUVECs was assessed by scratch test assay. As shown in Fig. 3D, after treatment with nano-Se for 12 h, the distance of cell migration continued to increase according to the concentration of Nano-Se. The migration rate of HUVECs reached 66.7% when the concentration of Nano-Se increased to 100 nM (Fig. 3E), while the migration rate remained at 53.3% in the control group. These results collectively indicated that angiogenesis-stimulated activity of Nano-Se is conserved between zebrafish and homo species.

Considering that angiogenesis improves the activity of Nano-Se in both zebrafish and human cells, we investigated whether fin regeneration improved by Nano-Se is dependent on Nano-Se-induced angiogenesis. A VEGFR2/KDR inhibitor, PTK787, was introduced to exclude angiogenesis by blocking VEGFR2 signaling, and the results showed that the regeneration rate, which was elevated with Nano-Se treatment, decreased when exposed to PTK787. Moreover, the enhancing activities of Nano-Se on both fin regeneration and angiogenesis were blocked in the presence of PTK787, indicating that VEGFR2 signaling is critical for Nano-Se-induced fin regeneration (Fig. 4). Collectively, these results indicated that Nano-Se improved fin regeneration through the induction of VEGFR2-mediated angiogenesis.

2.4. *Nano-Se promotes tissue regeneration through FGF and the Wnt/β-Catenin pathway*

In addition to blood vessels, stromal growth is also crucial for fin regeneration [45]. According to our RNA-Seq results (Fig. 1H), the FGF and Wnt/β-Catenin pathways were also involved in tissue regeneration promoted by Nano-Se. AZD4547 (FGFR inhibitor) and LGK974 (Wnt/β-Catenin inhibitor) were introduced to block the FGF and Wnt pathways to further evaluate their importance during fin regeneration stimulated by Nano-Se. As shown in Fig. 5 and 14 days after amputation, the fin regeneration rate, which was improved by Nano-Se, decreased when exposed to AZD4547. Moreover, the enhancing activities of Nano-Se on both fin regeneration and angiogenesis were blocked in the presence of AZD4547. LGK974 was introduced to exclude stromal

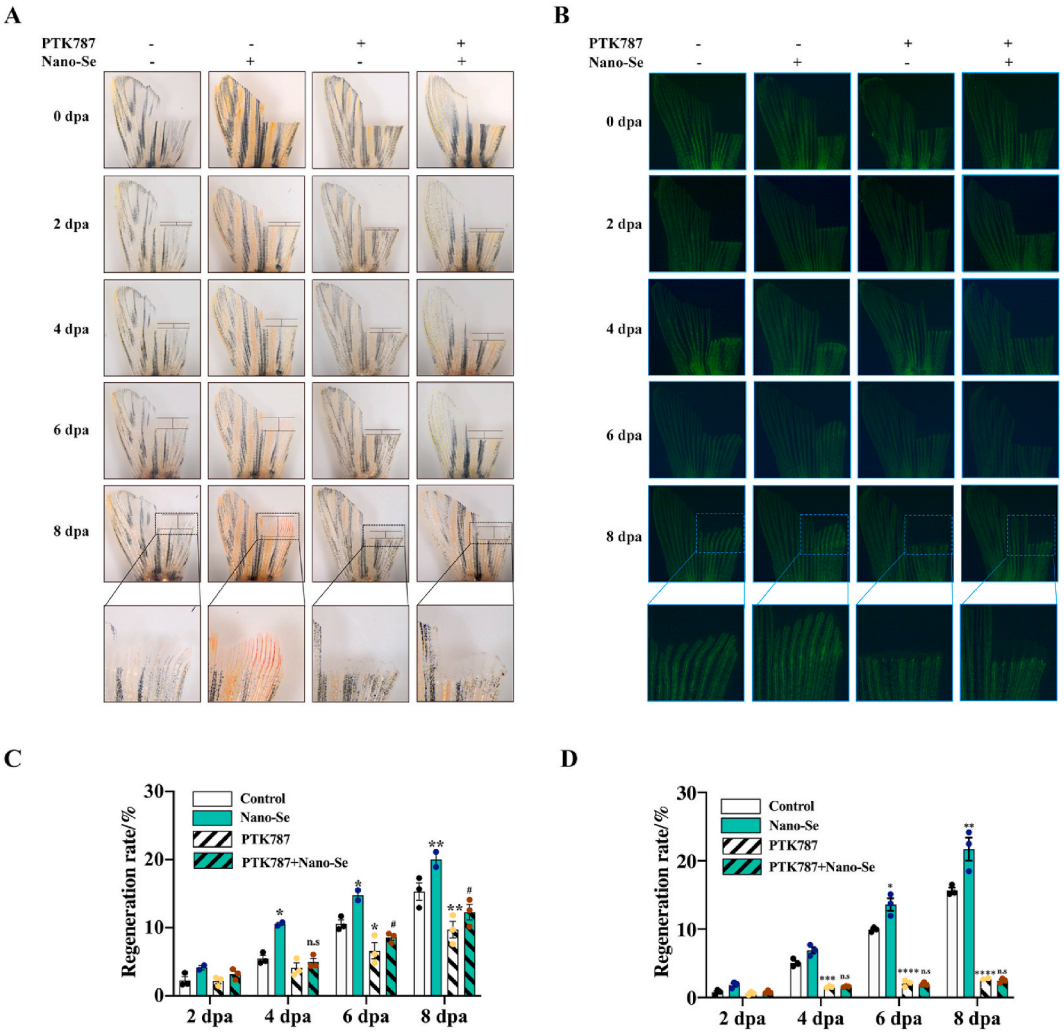

Fig. 4. **(A)** Representative images for caudal fin regeneration in adult zebrafish, the adult zebrafish were treated with Nano-Se (100 nM) and PTK787 (100 nM) (an inhibitor of VEGFR2/KDR). **(B)** Representative fluorescence microscopy images for angiogenesis in caudal fin by transgenosis zebrafish *(fli1:EGFP)*, the adult zebrafish were treated with Nano-Se (100 nM) and PTK787 (100 nM) (an inhibitor of VEGFR2/KDR) **(C)** Regeneration rate of caudal fin regeneration treated with Nano-Se (3 independent biological repeats with a total n = 13). **(D)** Angiogenesis rate of caudal fin treated with Nano-Se (3 independent biological repeats with a total n = 13). (Mean values ± SD, * : Significant difference compared with control group, *P < 0.05, **P < 0.01, ***P < 0.001, ****P < 0.0001, **#:** Significant difference between PTK787 and PTK787+ Nano-Se group, #P < 0.05, ##P < 0.01, ###P < 0.001, ####P < 0.0001, n.s: not significant difference between PTK787 and PTK787+ Nano-Se group, N.S: Not significant difference compared with control group).

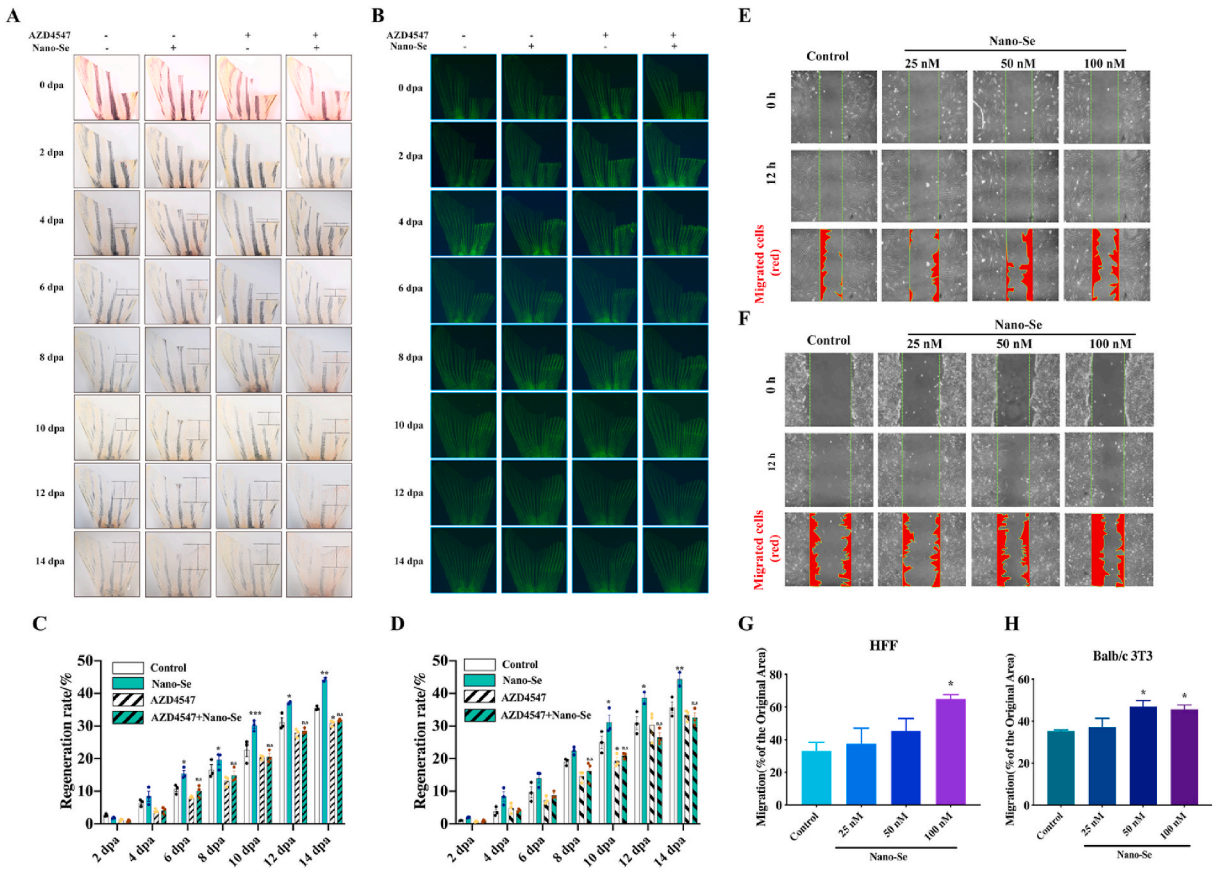

Fig. 5. **(A)** Representative images for caudal fin regeneration in adult zebrafish, the adult zebrafish were treated with Nano-Se (100 nM) and AZD4547 (50 nM) (an inhibitor of FGFR). **(B)** Representative fluorescence microscopy images for angiogenesis in caudal fin by transgenosis zebrafish (*fli1:EGFP*), the adult zebrafish were treated with Nano-Se (100 nM) and AZD4547 (50 nM) (an inhibitor of FGFR) **(C)** Regeneration rate of caudal fin regeneration treated with Nano-Se (4 independent biological repeats with a total n = 15). **(D)** Angiogenesis rate of caudal fin treated with Nano-Se (4 independent biological repeats with a total n = 15). **(E)** Wound healing assay to evaluate the migration of HFF cells after being treated with Nano-Se (0, 25, 50 and 100 nM) and DMEM with 10% FBS. Cells were wounded and monitored using a microscope 12 h. The red areas represent migrating cells. **(F)** Wound healing assay to evaluate the migration of Balb/c 3T3 cells after being treated with Nano-Se (0, 25, 50 and 100 nM) and DMEM with 10% FBS. Cells were wounded and monitored using a microscope 12 h. The red areas represent migrating cells. **(G)** Migration rate of HFF cells induced by Nano-Se (3 independent biological repeats with a total n = 9). **(H)** Migration rate of Balb/c 3T3 cells induced by Nano-Se (3 independent biological repeats with a total n = 9). (Mean values ± SD, * : Significant difference compared with control group, *P < 0.05, **P < 0.01, ***P < 0.001, ****P < 0.0001, **#**: Significant difference between AZD4547 and AZD4547+ Nano-Se group, #P < 0.05, ##P < 0.01, ###P < 0.001, ####P < 0.0001, n.s: not significant difference between AZD4547 and AZD4547+ Nano-Se group, N.S: Not significant difference compared with control group).

growth by blocking Wnt signaling, and the results showed that the fin regeneration rate, which was elevated with Nano-Se treatment, decreased when exposed to LGK974. Moreover, the enhancing activities of Nano-Se on both fin regeneration and angiogenesis were blocked in the presence of LGK974 at 6 days postamputation (Fig. 6). These results indicate that Nano-Se improves fin regeneration through the induction of FGFR and Wnt pathway-mediated stromal growth.

To investigate whether the stromal growth-enhancing activities of Nano-Se are conserved in mammals, human foreskin fibroblast cells (HFFs) and mouse embryonic fibroblast adherent cells (Balb/c 3T3) were employed for further investigation. The proliferation rate of Balb/c 3T3 cells was significantly increased after treatment with Nano-Se for 72 h (Fig. S12) while the LD50 of Nano-Se was 828.3 nM (Fig. S13B) . Moreover, the migration of HFF-fed and Balb/c 3T3 cells was assessed by scratch assays. After treatment with Nano-Se for 12 h, a decreased distance of wound closure was observed in HFF cells and Balb/c 3T3 cells (Fig. 5E and F). The migration rates of HFF cells and Balb/c 3T3 cells reached 60.9% and 45.8%, respectively, while the migration rate remained at 35.5% in the control group (Fig. 5G and H). These results collectively indicate that stromal growth-stimulated Nano-Se activity is conserved between zebrafish and homo species.

2.5. *Nano-Se promotes fin regeneration in hyperglycemic zebrafish*

Hyperglycemia contributes to disorders in tissue regeneration. We established a hyperglycemic zebrafish model through an overdiet accompanied by STZ injection (Fig. S14) to evaluate whether Nano-Se could improve fin regeneration under hyperglycemic conditions. As shown in Fig. 7A, the fin regeneration rate significantly decreased when the zebrafish entered hyperglycemic conditions. As the quantification results are shown in Fig. 7C, the fin regeneration rate dropped to 32.78% in hyperglycemic zebrafish compared to 48.85% in healthy zebrafish at 9 dpa, suggesting that hyperglycemia disturbed fin regeneration in zebrafish. Interestingly, Nano-Se also significantly promoted fin regeneration in hyperglycemic zebrafish (Fig. 7B and D). Our results demonstrate that Nano-Se can improve fin regeneration under hyperglycemic conditions.

The effect of Nano-Se on tissue regeneration was also verified in mammalian diabetic rats. As shown in Fig. 7E, the skin wound healing rate was significantly accelerated. Quantification results demonstrated that the wound healing rate with 4-day exposure to Nano-Se achieved a regeneration rate of 16.19% compared to that of 5.54% in the control group; this difference continued growing, and until 10-day Nano-Se exposure, the wound healing rate reached 76.0%, while the control

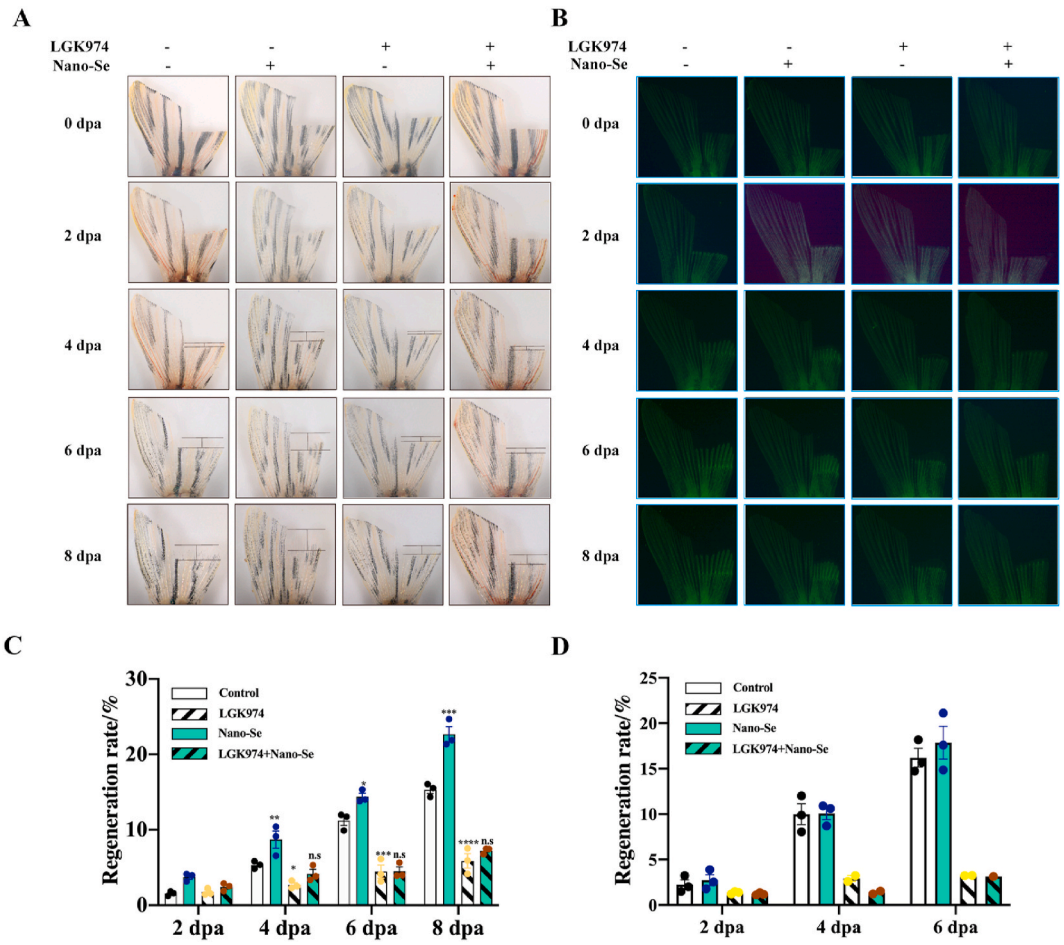

Fig. 6. **(A)** Representative images for caudal fin regeneration in adult zebrafish, the adult zebrafish were treated with Nano-Se (100 nM) and LGK974 (10 nM) (an inhibitor of Wnt pathway). **(B)** Representative fluorescence microscopy images for angiogenesis in caudal fin by transgenosis zebrafish *(fli1:EGFP)*, the adult zebrafish were treated with different concentrations of Nano-Se (100 nM) and LGK974 (10 nM) (an inhibitor of Wnt pathway) **(C)** Regeneration rate of fin regeneration treated with Nano-Se (3 independent biological repeats with a total n = 12). **(D)** Angiogenesis rate of transgenosis fin treated with Nano-Se (3 independent biological repeats with a total n = 12). (Mean values ± SD, * : Significant difference compared with control group, *P < 0.05, **P < 0.01, ***P < 0.001, ****P < 0.0001, #: Significant difference between LGK974 and LGK974+ Nano-Se group, #P < 0.05, ##P < 0.01, ###P < 0.001, ####P < 0.0001, n.s: not significant difference between LGK974 and LGK974+Nano-Se group, N.S: Not significant difference compared with control group).

group showed only 54.71% (Fig. 7F).

2.6. The toxicity effects of Nano-Se on zebrafish

To test the toxicity of Nano-Se used, zebrafish embryos were employed, and the results demonstrated that both the mortality rate and hatching rates revealed negligible acute toxicity after exposure to different concentrations of Nano-Se (Fig. S15). In addition to acute toxicity, the toxicity of nano-Se against adult zebrafish was also evaluated, and the body length and weight of adult zebrafish remained unchanged in the presence of nano-Se (Figs. S15G and S15F). These results indicate that nano-Se exhibits a fin regeneration-promoting effect at nontoxic doses and that the toxicity is lower than that of selenium salt (Fig. S16).

3. Discussion

The correlation of Se and tissue regeneration has been issued; however, there is still no direct or solid evidence regarding whether Se could benefit and how Se benefits tissue regeneration. Herein, we demonstrated that nano-Se promotes tissue regeneration at a nontoxic dose *in vivo* and *in vitro*. The regeneration-stimulating activities of Nano-Se are conserved across nonmammalian vertebrates (zebrafish), rodents (rats), and primates (human cells). Mechanistically, VEGFR signaling-mediated angiogenesis and Wnt/FGFR signaling-mediated stromal growth play crucial roles during tissue regeneration accelerated by Nano-Se. Moreover, our results demonstrated that Nano-Se also benefits the regeneration of refractory wounds in hyperglycemic animals, including zebrafish and rats. Our results highlight Nano-Se as a potential candidate for tissue regeneration-related disorders, including hyperglycemia-related refractory wounds.

Epidemiological studies have suggested the correlation of Se deficiency and poor prognosis of the spinal cord [46] and liver regeneration [47]. However, there is still no direct evidence that selenium benefits tissue regeneration. This study is one of the leading investigations that revealed the tissue regeneration stimulating activity of Nano-Se. Recently, Nano-Au-containing hydrogels [48,49] demonstrated antibacterial activity [50] and thus accelerated tissue regeneration. However, Nano-Au also inhibits VEGF-induced choroid-retina endothelial cell migration [51], which is critical for tissue regeneration. Another nanomaterial, sulfur nanoparticles (Nano-S), also demonstrated excellent antibacterial activity [52–54], which plays a positive role during tissue regeneration. In our study, neither Nano-Au nor Nano-S (100 nm, almost the same size as Nano-Se) significantly promoted tissue regeneration. One of the probable reasons is that bacterial infection is negligible around the wound. Selenite also did not exhibit a significant effect

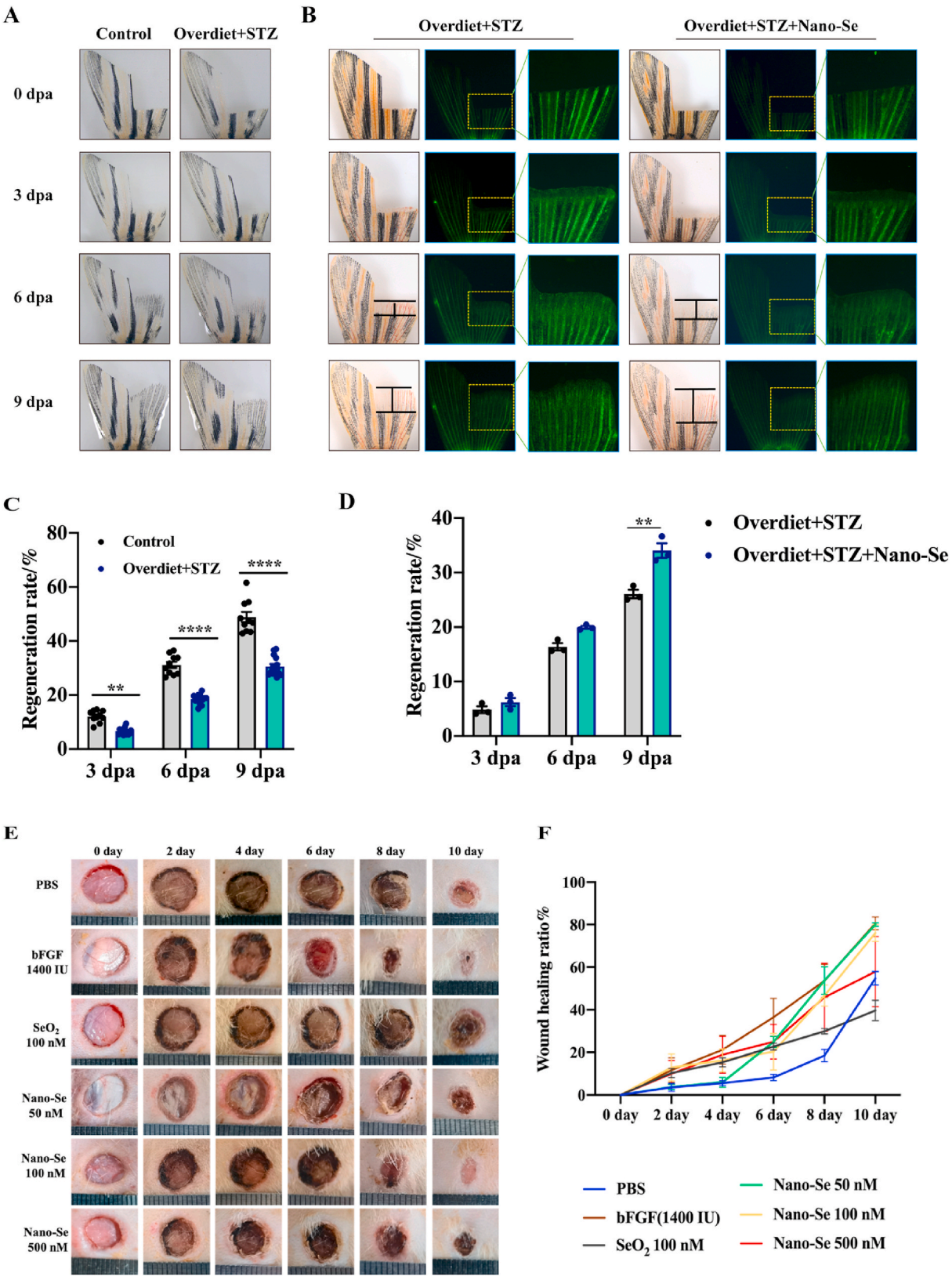

Fig. 7. **(A)** Representative images for zebrafish caudal fin regeneration by overdiet (6 times a day) and intraperitoneal injection of streptozocin (STZ); **(B)** Representative images for caudal fin regeneration by overdiet and intraperitoneal injection STZ with transgenosis zebrafish *(coroa1: EGFP)* which inflammatory cells are labeled with green fluorescence, the adult zebrafish were treated with Nano-Se (100 nM); **(C)** Regeneration rate of fin regeneration treated with overdiet and STZ (3 independent biological repeats with a total n = 24). **(D)** Regeneration rate of fin regeneration treated with Nano-Se (3 independent biological repeats with a total n = 12). **(E)** Representative images of Nano-Se in a dorsal cortex injury SD diabetic rats model. **(F)** Wound healing rate of Nano-Se in a dorsal cortex injury SD diabetic rats model (3 independent biological repeats with a total n = 15). (Mean values ± SD, *P < 0.05, **P < 0.01, ***P < 0.001, ****P < 0.0001).

on tissue regeneration, which may be attributed to its low bioavailability [55]. Nano-Se has been extensively investigated due to its antioxidative, anticancer, and anti-inflammatory activities; however, Nano-Se exhibited these activities at the toxic dose [56–58]. The regeneration accelerating activity of Nano-Se is exerted at a nontoxic dose range according to this study, which demonstrated the unique property of Nano-Se for tissue regeneration.

Tissue regeneration is a complex process involving multiple cell types and various signaling pathways. The signaling pathways involved in tissue regeneration mainly include WNT [59], FGF [60], IGF [61], BMP [62], Notch [63], Hippo [64], Hedgehog [65], and VEGF [66]. The cell types involved in regeneration depend on the type of regenerating tissue. For instance, skin regeneration can be roughly divided into stromal regeneration and angiogenesis [67]. In this study, we found that WNT and FGF signaling were involved in and crucial for Nano-Se-induced stromal growth. The importance of these two signaling pathways has been stressed in zebrafish and mouse studies [68,69]. Thus, the results of our study are consistent with previous investigations. In addition, angiogenesis is vital for tissue regeneration. Angiogenesis is usually driven by VEGFs, a subset of well-known growth factors [70]. Our results also indicate that Nano-Se promoted angiogenesis in a VEGF signaling-dependent manner, consistent with previous studies. Taken together, Nano-Se accelerated tissue regeneration through classical WNT/FGF signaling-induced stromal growth and VEGF signaling-induced angiogenesis.

Skin is one of the regenerable organs in adults; however, it also demonstrates regeneration disorders under pathological situations, such as diabetic feet [71]. According to clinical statistics, approximately 25% of patients with severe hyperglycemia have refractory wounds, mainly diabetic feet, which is currently a bottleneck in the clinic [72]. Our results revealed that Nano-Se benefits regeneration in hyperglycemia-related refractory wounds in both zebrafish and rat models. There are several approaches to establish a hyperglycemia model in zebrafish [73]. Herein, we combined STZ intraperitoneal injection and overdiet to induce severe hyperglycemia in models. One of the reasons is that diabetic feet mainly occur in severe diabetic patients, in which the β-cells have already been distorted (type I) or exhausted (type II). STZ reduces the functions of β-cells, while an overdiet accelerates the accumulation of blood sugar [74]. By combining these two approaches, we established hyperglycemia-related refractory wounds in both zebrafish and rat models, which are similar to clinical patients. In this manner, we showed that Nano-Se benefits regeneration in hyperglycemia-related refractory wounds *in vivo*.

Taken together, we highlighted Nano-Se as an accelerator for tissue regeneration under both physiological and pathological conditions at its nontoxic doses. Mechanistically, Nano-Se triggers WNT/FGF signaling-dependent stromal growth and VEGF signaling-dependent angiogenesis, which is one of the classical mechanisms during tissue regeneration (Fig. 8). Our findings support the regeneration-promoting activity of Nano-Se, especially in diabetic patients.

4. Conclusion

In summary, we illustrated PEG modification methods for hydrosoluble Nano-Se synthesis. By zebrafish screening, we first reported that Nano-Se not only promotes tissue regeneration through the VEGFR, FGFR and Wnt signaling pathways but also promotes the repair of skin under hyperglycemic conditions, and the effect of Nano-Se on tissue regeneration in diabetic rats was verified. This work demonstrates the possibility of applying PEG modification to synthesize hydrosoluble nano-Se and, more importantly, provides zebrafish as an *in vivo* model for screening the novel biological activity of nanomaterials. This research is not only the first discovery of a new function of Nano-Se: promoting tissue regeneration; it also provides a new treatment idea for the regeneration of clinical skin tissue. In future work, we will conduct in-depth research on the appropriate pharmaceutical formulations and toxic effects of Nano-Se to provide a foundation for human clinical therapy.

5. Materials and methods

5.1. Materials

Selenium (Se), sulfur (S), MS-222,6-coumarin and streptozocin (STZ) were purchased from Sigma–Aldrich Chemical Co., PEG200 was purchased from Sangon Biotech Co. Ltd. and used without further purification. PTK787, AZD4547, and LGK974 were purchased from MedChem Express Co. DMEM was purchased from Gibco Co. Ltd. FBS was purchased from Biological Industries Co. Ltd. The BeyoClick™ EdU Cell Proliferation Kit was purchased from Beyotime Biotechnology Co., Ltd. Ultrapure Milli-Q water was used in all experiments.

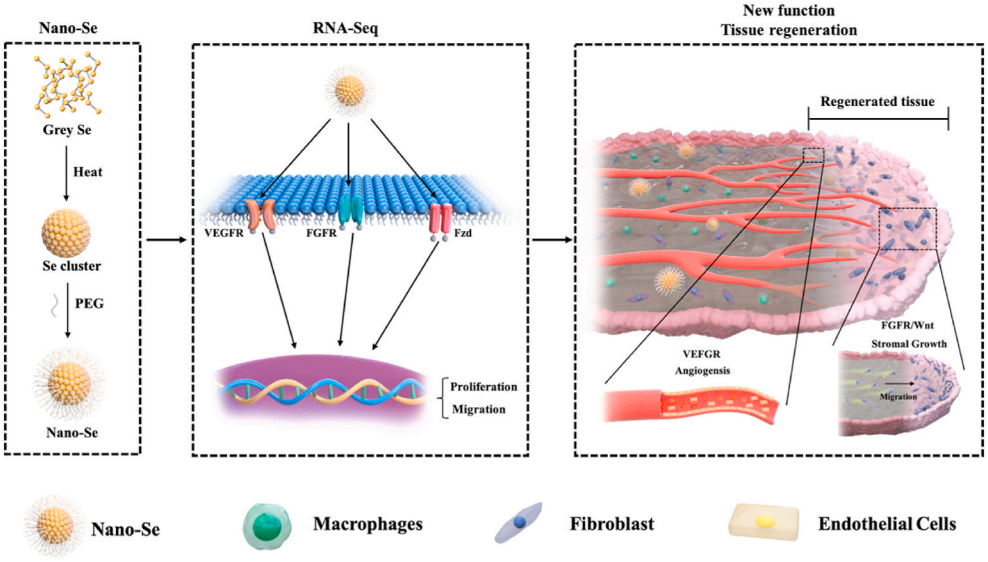

Fig. 8. Diagram of the tissue regeneration accelerated by Nano-Se through promoting stromal growth by FGFR/Wnt signal pathway and angiogenesis by VEGFR signal pathway.

5.2. Cell lines

Cell lines, including human umbilical vein endothelial HUVECs, human skin fibroblast HFFs, and mouse embryonic fibroblast Balb/c 3T3 cells, were purchased from American Type Culture Collection (ATCC, Manassas, VA, USA).

5.3. Zebrafish transgenic lines and zebrafish maintenance

The transgenic line (*fli1*: *EGFP/gata1*: mCherry), in which blood vessels were labeled with green fluorescence and blood was labeled with red fluorescence, was used to observe fin blood vessel regeneration. The transgenic line (*coro1a*: EGFP) in which inflammatory cells are labeled with green fluorescence was used to observe the fin regeneration rate of Nano-Se-treated hyperglycemic zebrafish. Adult zebrafish were maintained in a water circulation system, the water temperature was maintained at 28 °C, the conductivity was adjusted to 500–550, and the pH of the culture water was adjusted to 7.5–8.0.

5.4. Synthesis and Characterization of Nano-Se

Nano-Se was synthesized by dissolving 20 mg of gray Se powder in 10 mL of PEG200 solution under magnetic stirring for 15 min at room temperature when the solution turned from colorless to dark brown, but there was still a large amount of gray selenium at the bottom of the solution. Next, the dark brown solution was incubated at 200–220 °C for 30 minutes to observe that the solution became red brown and that the gray selenium was completely dissolved. Then, an equal volume of water (4 °C) was immediately added to the reaction solution, and the reaction solution was brown-red to rose-red. Finally, the solution was filtered with a 0.22 μm filter membrane to obtain a red Nano-Se solution.

Transmission electron microscopy (TEM) samples were prepared by dispersing the samples onto a holey carbon film on copper grids. The micrographs were obtained on a Tecnai G220 (Shimadzu, Japan) at 200 keV. A dynamic light scattering (DLS) particle size analyzer (Malvern 2000, USA) was used to determine the hydrophilic diameters of the particles. The concentration of Se was detected by inductively coupled plasma-atomic emission spectrometry (ICP-AES) (Thermo Scientific, iCAP 7400, USA). All the measurements were performed at room temperature if not specially mentioned.

5.5. Zebrafish fin regeneration model

Wild-type adult zebrafish and transgenic adult zebrafish (4–8 months old) were anesthetized in 0.1% MS-222, and caudal fins were amputated using a scalpel. Then, the experimental group was treated with Nano-Se every other day for 8 days. Finally, zebrafish were anesthetized with 0.1% MS-222, and fin regeneration length was collected by fluorescence microscopy (Mingmei Optoelectronics Technology Co. Ltd.) for analysis at different time points. Regeneration rate of zebrafish caudal fin treated with Nano-Se. (3 independent biological repeats with a total n = 29); Regeneration rate of adult zebrafish caudal fin treated with Nano-S, Nano-Au, Nano-Se (3 independent biological repeats with a total n = 15); Regeneration rate of fin angiogenesis treated with Nano-Se through VEGFR (3 independent biological repeats with a total n = 13); Regeneration rate of caudal fin regeneration treated with Nano-Se through FGFR; (4 independent biological repeats with a total n = 15); Regeneration rate of caudal fin regeneration treated with Nano-Se through Wnt pathway (3 independent biological repeats with a total n = 12). All animal experiments complied with the Arrive guidelines and were carried out in accordance with the National Institutes of Health Guide for the Care and Use of Laboratory Animals.

5.6. Skin wound healing model of SD rats

SD rats were provided by Guangdong Medical Laboratory Animal Center. Adult SD rats were anesthetized with pentobarbital sodium. After the rats were anesthetized, a skin perforator with a diameter of 8 mm was used to construct a skin wound healing model on the backs of the rats. After the wound healing model was constructed, different concentrations of nano selenium were administered subcutaneously at the wound site. Acquired images and ImageJ were used to quantify the wound healing rate based on five different fields of vision. (3 independent biological repeats with a total n = 15).The animals were maintained in accordance with the Guide for the Care and Use of Laboratory Animals issued by the National Institutes of Health and approved by the Laboratory Animal Ethics Committee of Jinan University.

5.7. Extraction and purification of total RNA from zebrafish regenerated fin tissue and bioinformatics analysis

After tail-cutting 30 wild-type (WT) zebrafish, they were randomly divided into two groups: one group was cultured in system aquaculture (control group, n = 15), and the other group was treated with Nano-Se (100 nM) every other day for 8 days. Then, the regenerated fins were collected. Total RNA was obtained with an RNeasy Micro Kit according to standard operating procedures. After electrophoresis, the RNAClean XP Kit and RNase-Free DNase Set were used to purify total RNA. Only high-quality RNA samples (OD260/280 = 1.8–2.0, RIN ≥9.5, 28S:18S = 1.6–2.4) were used to construct a sequencing library, Illumina HiSeq X10 was used, and RNA purification was performed at Shanghai Bohao Biotechnology Co. Ltd. reverse transcription, library construction, and sequencing. For bioinformatics analysis, the expression level of each transcript was calculated based on the number of fragments per million exons per million map reading (FPKM) method. RSEM is used to quantify gene abundance. The R statistical software package DESeq2 (fold change ≥2 and P value < 0.05) was used to identify differentially expressed genes, with a false discovery rate (FDR) cutoff value < 0.05. KEGG functional enrichment analysis showed that differentially expressed genes were significantly enriched in the KEGG signaling pathway. KEGG enrichment analysis was performed by KOBAS 2.1.1.

5.8. Localization of Nano-Se in the caudal fin of adult zebrafish

Nano-Se was labeled with 6-coumarin with green fluorescence. Wild-type adult zebrafish (4–8 months old) were anesthetized in 0.1% MS-222, and caudal fins were amputated using a scalpel and treated with Nano-Se@6-coumarin for 1 hour. Then, Nano-Se@6-coumarin was removed, and the distribution of green fluorescence in the tail fin of zebrafish was collected at different time points.

5.9. Scratch test assay

The digested cells were inoculated at a dilution of 4×10^4 cells/well into a six-well plate, incubated in a 37 °C 5% CO_2 incubator for 24 hours to form a monolayer, and then treated with DMEM (0.5% FBS) for 12 h for starvation. A line was then scratched on the culture using a tip (200 μL pipet) orthogonal to the mark on the plate, and the six-well plate was shaken carefully with PBS to remove floating or dead cells. Nano-Se was diluted with 0.5% starvation medium to different concentrations, and the same volume was added to each well and cultured for 24 hours. Images were acquired with a microscope, and ImageJ was used to quantify cell migration activity. The average migration rate was calculated based on five different fields of vision. (3 independent biological repeats with a total n = 9).

5.10. CCK8 assay

The digested cells were inoculated at a dilution of 2×10^3 cells/well into a 96-well plate and incubated in a 37 °C 5% CO_2 incubator for 24 hours. Then, the cells were treated with DMEM (0.5% FBS) for 24 h for starvation and to remove the medium. Nano-Se was diluted with 0.5%

starvation medium to different concentrations, and the same volume was added to each well. The cells were cultured for 48 hours, and the medium was removed. Next, 100 μL/well CKK-8 solution was added for 1 h. Finally, the absorbance of each well at 450 nm was measured with a microplate analyzer. (3 independent biological repeats with a total n = 9).

5.11. *In vitro cytotoxicity of Nano-Se*

HUVECs and HFF cell lines were used to evaluate the *in vitro* toxicity of Nano-Se. The dose of Nano-Se was set at 0, 0.625, 1.25, 2.5, and 5 μM, and the *in vitro* toxicity of Nano-Se was determined by the CCK-8 assay (5.10 for the experimental method). Finally, PRISM software was used to calculate the LD50 of nano-Se with three replicates in each group.

5.12. *BeyoClick™ EdU assay*

A total of 3×10^3 cells/mL were added to a 12-well plate, incubated in a 37 °C 5% CO2 incubator for 12 hours, treated with DMEM (0.5% FBS) for 24 h for starvation and medium removal. Then, the cells were treated with different concentrations of Nano-Se for 48 hours. Finally, the cells were treated according to the instructions of the BeyoClick™ EdU kit, and five different fields of view were randomly selected to determine the cell proliferation rate. Proliferation rate = number of proliferating cells/total number of cells × 100%

5.13. *Establishment of a hyperglycemic zebrafish tail fin regeneration model*

Adult zebrafish were anesthetized and divided into two groups: the control group (2 times a day) and the overeating (6 times a day) + STZ group (injected once every other day for the first two weeks and once a week for the next two weeks with a high-fat diet) (3 independent biological repeats with a total n = 24). When it lasted for a month, a scalpel was used to cut off a quarter of the zebrafish tail from the bifurcation to successfully construct a cut tail model. Then, the zebrafish were treated with Nano-Se (100 nM) (3 independent biological repeats with a total n = 12). Finally, adult zebrafish were anesthetized, and fin tail regenerates were collected by fluorescence microscopy (Mingmei Optoelectronics Technology Co., Ltd.) for analysis at different time points.

5.14. *Evaluation of nanose on the developmental toxicity of zebrafish*

Wild-type juvenile zebrafish (24 hours after fertilization) were placed into 24-well plates, and each well contained 10 strips. Then, Nano-Se was treated with 0 nM, 50 nM, 100 nM, and 200 nM every other day. The number of zebrafish that survived and hatched in each well was recorded every 24 hours until 96 hours. The heartbeat of each zebrafish in each group was counted (times/min), and the zebrafish body length in each group was measured at 96 hours. Adult wild-type zebrafish were divided into two groups and treated with 0 nM or 100 nM Nano-Se every other day for 8 days. Finally, the length and weight of zebrafish in each group were collected.

5.15. *Statistical analysis*

The data are expressed as the mean ± standard deviation (SD). Data were analyzed using GraphPad Prism 8.0 software (one-way ANOVA or two-way ANOVA, (*) for $p < 0.05$, (**) for $p < 0.01$, (***) for $p < 0.001$, and (****) for $p < 0.0001$).

Ethics statement

This study was approved by the research ethics committee of Jinan University.

Credit author statement

Jieqiong Cao: Conceptualization, Methodology, Formal analysis, Writing-original draft and review. **Yibo Zhang:** Conceptualization, Formal analysis, Writing-review. **Peiguang Zhang:** Methodology. **Zilei Zhang:** Methodology. **Bihui Zhang:** Methodology. **Yanxian Feng:** Conceptualization, Methodology. **Zhixin Li:** Methodology. **Yiqi Yang:** Methodology. **Qilin Meng:** Methodology. **Liu He:** Formal analysis. **Yulin Cai:** Formal analysis. **Zhenyu Wang:** Formal analysis. **Jie Li:** Formal analysis. **Xue Chen:** Formal analysis. **Hongwei Liu:** Formal analysis. **An Hong:** Conceptualization, Formal analysis, Funding acquisition. **Wenjie Zheng:** Conceptualization, Supervision, Formal analysis. **Xiaojia Chen:** Conceptualization, Formal analysis, Writing-review, Project administration.

Declaration of competing interest

The authors declare that there is no conflict of interest.

Acknowledgments

This study was supported by grants from National Natural Science Foundation of China (No. 81902801), National Natural Science Foundation of China (No.8217329), Operating Fund of Guangdong Provincial Key Laboratory of Bioengineering Medicine (No. 2014B030301050), Guangdong grant “Key technologies for treatment of brain disorders” (No.2018B030332001), China Postdoctoral Foundation (No.2019M663375), Guangzhou Science and Technology Project (No.20212210007) and the authors especially thank to Dr. Wangxiao He (Xi’an Jiaotong University) for revising the article.

Appendix A. Supplementary data

Supplementary data to this article can be found online at https://doi.org/10.1016/j.bioactmat.2021.12.026.

References

[1] A. Kumar, K.S. Prasad, Role of nano-selenium in health and environment, J. Biotechnol. 325 (2021) 152–163, https://doi.org/10.1016/j.jbiotec.2020.11.004.
[2] L.M. Ensign, R. Cone, J. Hanes, Oral drug delivery with polymeric nanoparticles: the gastrointestinal mucus barriers, Adv. Drug. Deliv. Rev. 64 (2012) 557–570.
[3] B. Hosnedlova, M. Kepinska, S. Skalickova, C. Fernandez, B. Ruttkay-Nedecky, Q. Peng, M. Baron, M. Melcova, R. Opatrilova, J. Zidkova, G. Bjorklund, J. Sochor, R. Kizek, Nano-selenium and its nanomedicine applications: a critical review, Int. J. Nanomedicine. 13 (2018) 2107–2128, https://doi.org/10.2147/IJN.S157541.
[4] J. Zhang, J.E. Spallholz, Toxicity of selenium compounds and nano-selenium particles, in: B. Ballantyne, T.C. Marrs, T. Syversen, D.A. Casciano, S.C. Sahu (Eds.), General, Applied and Systems Toxicology, 2011, https://doi.org/10.1002/9780470744307.gat243.
[5] L. Shi, W. Xun, W. Yue, C. Zhang, Y. Ren, L. Shi, Q. Wang, R. Yang, F. Lei, Effect of sodium selenite, Se-yeast and nano-elemental selenium on growth performance, Se concentration and antioxidant status in growing male goats, Small Rumin. Res. 96 (2011) 49–52, https://doi.org/10.1016/j.smallrumres.2010.11.005.
[6] S.K. Torres, V.L. Campos, C.G. León, S.M. Rodríguez-Llamazares, S.M. Rojas, M. González, C. Smith, M.A. Mondaca, Biosynthesis of selenium nanoparticles by Pantoea agglomerans and their antioxidant activity, J. Nanopart. Res. 14 (2012) 1236, https://doi.org/10.1007/s11051-012-1236-3.
[7] L. Yuan, X. Yin, Y. Zhu, L. Fei, H. Yang, L. Ying, Z. Lin, Selenium in Plants and Soils, and Selenosis in Enshi, China: Implications for Selenium Biofortification, Springer Netherlands, 2012, https://doi.org/10.1007/978-94-007-1439-7_2.
[8] N. Hadrup, G. Ravn-Haren, Acute human toxicity and mortality after selenium ingestion: a review, Journal of Trace Elements in Medicine and Biology 58 (2019) 126435, https://doi.org/10.1016/j.jtemb.2019.126435.
[9] W.P. Fang, Y.T. Cheng, Y.R. Cheng, Y.J. Cherng, Synthesis of substituted uracils by the reactions of halouracils with selenium, sulfur, oxygen and nitrogen nucleophiles under focused microwave irradiation, Cheminform 61 (2005) 3107–3113, https://doi.org/10.1016/j.tet.2005.01.085.
[10] R. Bakalova, Z. Zhelev, R. Jose, T. Nagase, H. Ohba, M. Ishikawa, Y. Baba, Role of free cadmium and selenium ions in the potential mechanism for the enhancement of photoluminescence of CdSe quantum dots under ultraviolet irradiation, Journal of Nanoscience & Nanotechnology 5 (2005) 887–894, https://doi.org/10.1166/jnn.2005.117.

[11] M. Quintana, E. Haro-Poniatowski, J. Morales, N. Batina, Synthesis of selenium nanoparticles by pulsed laser ablation, Applied Surface Science 195 (2002) 175–186, https://doi.org/10.1016/S0169-4332(02)00549-4.
[12] X. Li, Y. Li, S. Li, W. Zhou, H. Chu, W. Chen, I.L. Li, Z. Tang, Single crystalline trigonal selenium nanotubes and nanowires synthesized by sonochemical process, Crystal Growth & Design 5 (2005) 911–916, https://doi.org/10.1021/cg049681q.
[13] B. Deng, J. Feng, J. Meng, Speciation of inorganic selenium using capillary electrophoresis-inductively coupled plasma-atomic emission spectrometry with on-line hydride generation, Anal Chim Acta 583 (2007) 92–97, https://doi.org/10.1016/j.aca.2006.09.038.
[14] M. Pettine, F. Gennari, L. Campanella, The reaction of selenium (IV) with ascorbic acid: its relevance in aqueous and soil systems, Chemosphere 90 (2013) 245–250, https://doi.org/10.1016/j.chemosphere.2012.06.061.
[15] M.A.O. Dawood, M. Zommara, N.M. Eweedah, A.I. Helal, M.A. Aboel-Darag, The potential role of nano-selenium and vitamin C on the performances of Nile tilapia (Oreochromis niloticus), Environ. Sci. Pollut. Res. Int. 27 (2020) 9843–9852, https://doi.org/10.1007/s11356-020-07651-5.
[16] S. Chung, R. Zhou, T.J. Webster, Green synthesized BSA-coated selenium nanoparticles inhibit bacterial growth while promoting mammalian cell growth, Int. J. Nanomedicine. 15 (2020) 115–124, https://doi.org/10.2147/IJN.S193886.
[17] K. Viacava, E. Ammann, D. Bravo, M. Lenz, Low-temperature reactive aerosol processing for large-scale synthesis of selenium nanoparticles, Industrial And Engineering Chemistry Research 59 (2020) 16088–16094, https://doi.org/10.1021/acs.iecr.0c03213.
[18] Y. Ye, J. Qu, Y. Pu, S. Rao, F. Xu, C. Wu, Selenium biofortification of crop food by beneficial microorganisms, J. Fungi. (Basel) 6 (2020) 59–74, https://doi.org/10.3390/jof6020059.
[19] X. Zhang, H. He, J. Xiang, H. Yin, T. Hou, Selenium-containing proteins/peptides from plants: a review on the structures and functions, J Agric Food Chem 68 (2020) 15061–15073, https://doi.org/10.1021/acs.jafc.0c05594.
[20] P.G. Jamkhande, N.W. Ghule, A.H. Bamer, M.G. Kalaskar, Metal nanoparticles synthesis: an overview on methods of preparation, advantages and disadvantages, and applications, Journal of Drug Delivery Science and Technology 53 (2019) 101174, https://doi.org/10.1016/j.jddst.2019.101174.
[21] K. Parveen, V. Banse, L. Ledwani, Green Synthesis of Nanoparticles: Their Advantages and Disadvantages, American Institute of Physics Conference Series, 2016.
[22] P. Korde, S.K. Ghotekar, T. Pagar, S. Pansambal, D. Mane, Plant Extract Assisted Eco-Benevolent Synthesis of Selenium Nanoparticles-A Review on Plant Parts Involved, Characterization and Their Recent Applications, 2020, p. 1724, https://doi.org/10.1063/1.4945168.
[23] B. Hosnedlova, M. Kepinska, S. Skalickova, C. Fernandez, B. Ruttkay-Nedecky, Q. M. Peng, M. Baron, M. Melcova, R. Opatrilova, J. Zidkova, G. Bjorklund, J. Sochor, R. Kizek, Nano-selenium and its nanomedicine applications: a critical review, International Journal of Nanomedicine 13 (2018) 2107–2128, https://doi.org/10.2147/Ijn.S157541.
[24] S. Dhanjal, S.S. Cameotra, Aerobic biogenesis of selenium nanospheres by Bacillus cereus isolated from coalmine soil, Microbial Cell Factories 9 (2010), https://doi.org/10.1186/1475-2859-9-52. Artn 52.
[25] L.D. Geoffrion, T. Hesabizadeh, D. Medina-Cruz, M. Kusper, P. Taylor, A. Vernet-Crua, J.J. Chen, A. Ajo, T.J. Webster, G. Guisbiers, Naked selenium nanoparticles for antibacterial and anticancer treatments, Acs Omega 5 (2020) 2660–2669, https://doi.org/10.1021/acsomega.9b03172.
[26] D.L. Zeng, J.F. Zhao, K.H. Luk, S.T. Cheung, K.H. Wong, T.F. Chen, Potentiation of in vivo anticancer efficacy of selenium nanoparticles by mushroom polysaccharides surface decoration, Journal of Agricultural and Food Chemistry 67 (2019) 2865–2876, https://doi.org/10.1021/acs.jafc.9b00193.
[27] S. Zeng, Y. Ke, Y. Liu, Y. Shen, L. Zhang, C. Li, A. Liu, L. Shen, X. Hu, H. Wu, W. Wu, Y. Liu, Synthesis and antidiabetic properties of chitosan-stabilized selenium nanoparticles, Colloids Surf. B. Biointerfaces 170 (2018) 115–121, https://doi.org/10.1016/j.colsurfb.2018.06.003.
[28] D. Rajendran, Application of nano minerals in animal production system, Research Journal of Biotechnology 8 (2013) 1–3.
[29] A. Khurana, S. Tekula, M.A. Saifi, P. Venkatesh, C. Godugu, Therapeutic applications of selenium nanoparticles, Biomed Pharmacother 111 (2019) 802–812, https://doi.org/10.1016/j.biopha.2018.12.146.
[30] M.C. Bibby, Orthotopic models of cancer for preclinical drug evaluation: advantages and disadvantages, European Journal of Cancer 40 (2004) 852–857, https://doi.org/10.1016/j.ejca.2003.11.021.
[31] C.A. MacRae, R.T. Peterson, Zebrafish as tools for drug discovery, Nat. Rev. Drug Discov. 14 (2015) 721–731, https://doi.org/10.1038/nrd4627.
[32] K. Howe, M.D. Clark, C.F. Torroja, J. Torrance, C. Berthelot, M. Muffato, J. E. Collins, S. Humphray, K. McLaren, L. Matthews, S. McLaren, I. Sealy, M. Caccamo, C. Churcher, C. Scott, J.C. Barrett, R. Koch, G.J. Rauch, S. White, W. Chow, B. Kilian, L.T. Quintais, J.A. Guerra-Assuncao, Y. Zhou, Y. Gu, J. Yen, J. H. Vogel, T. Eyre, S. Redmond, R. Banerjee, J. Chi, B. Fu, E. Langley, S.F. Maguire, G.K. Laird, D. Lloyd, E. Kenyon, S. Donaldson, H. Sehra, J. Almeida-King, J. Loveland, S. Trevanion, M. Jones, M. Quail, D. Willey, A. Hunt, J. Burton, S. Sims, K. McLay, B. Plumb, J. Davis, C. Clee, K. Oliver, R. Clark, C. Riddle, D. Elliot, G. Threadgold, G. Harden, D. Ware, S. Begum, B. Mortimore, G. Kerry, P. Heath, B. Phillimore, A. Tracey, N. Corby, M. Dunn, C. Johnson, J. Wood, S. Clark, S. Pelan, G. Griffiths, M. Smith, R. Glithero, P. Howden, N. Barker, C. Lloyd, C. Stevens, J. Harley, K. Holt, G. Panagiotidis, J. Lovell, H. Beasley, C. Henderson, D. Gordon, K. Auger, D. Wright, J. Collins, C. Raisen, L. Dyer, K. Leung, L. Robertson, K. Ambridge, D. Leongamornlert, S. McGuire, R. Gilderthorp, C. Griffiths, D. Manthravadi, S. Nichol, G. Barker, S. Whitehead, M. Kay, J. Brown, C. Murnane, E. Gray, M. Humphries, N. Sycamore, D. Barker, D. Saunders, J. Wallis, A. Babbage, S. Hammond, M. Mashreghi-Mohammadi, L. Barr, S. Martin, P. Wray, A. Ellington, N. Matthews, M. Ellwood, R. Woodmansey, G. Clark, J. Cooper, A. Tromans, D. Grafham, C. Skuce, R. Pandian, R. Andrews, E. Harrison, A. Kimberley, J. Garnett, N. Fosker, R. Hall, P. Garner, D. Kelly, C. Bird, S. Palmer, I. Gehring, A. Berger, C.M. Dooley, Z. Ersan-Urun, C. Eser, H. Geiger, M. Geisler, L. Karotki, A. Kirn, J. Konantz, M. Konantz, M. Oberlander, S. Rudolph-Geiger, M. Teucke, C. Lanz, G. Raddatz, K. Osoegawa, B. Zhu, A. Rapp, S. Widaa, C. Langford, F. Yang, S.C. Schuster, N.P. Carter, J. Harrow, Z. Ning, J. Herrero, S.M. Searle, A. Enright, R. Geisler, R.H. Plasterk, C. Lee, M. Westerfield, P.J. de Jong, L.I. Zon, J.H. Postlethwait, C. Nusslein-Volhard, T.J. Hubbard, H. Roest Crollius, J. Rogers, D.L. Stemple, The zebrafish reference genome sequence and its relationship to the human genome, Nature 496 (2013) 498–503, https://doi.org/10.1038/nature12111.
[33] G.J. Lieschke, P.D. Currie, Animal models of human disease: zebrafish swim into view, Nat Rev Genet 8 (2007) 353–367, https://doi.org/10.1038/nrg2091.
[34] M.I. Pronobis, S. Zheng, S.P. Singh, J.A. Goldman, K.D. Poss, In vivo proximity labeling identifies cardiomyocyte protein networks during zebrafish heart regeneration, Elife 10 (2021), https://doi.org/10.7554/eLife.66079.
[35] W.C. Chen, Z. Wang, M.A. Missinato, D.W. Park, D.W. Long, H.J. Liu, X. Zeng, N. A. Yates, K. Kim, Y. Wang, Decellularized zebrafish cardiac extracellular matrix induces mammalian heart regeneration, Sci Adv 2 (2016), e1600844, https://doi.org/10.1126/sciadv.1600844.
[36] J. Wan, D. Goldman, Retina regeneration in zebrafish, Curr Opin Genet Dev 40 (2016) 41–47, https://doi.org/10.1016/j.gde.2016.05.009.
[37] C.N. Kamei, T.F. Gallegos, Y. Liu, N. Hukriede, I.A. Drummond, Wnt signaling mediates new nephron formation during zebrafish kidney regeneration, Development 146 (2019), https://doi.org/10.1242/dev.168294.
[38] T.F. Gallegos, C.N. Kamei, M. Rohly, I.A. Drummond, Fibroblast growth factor signaling mediates progenitor cell aggregation and nephron regeneration in the adult zebrafish kidney, Dev Biol 454 (2019) 44–51, https://doi.org/10.1016/j.ydbio.2019.06.011.
[39] J. So, M. Kim, S.H. Lee, S. Ko, D.A. Lee, H. Park, M. Azuma, M.J. Parsons, D. Prober, D. Shin, Attenuating the epidermal growth factor receptor-extracellular signal-regulated kinase-sex-determining region Y-box 9 Axis promotes liver progenitor cell-mediated liver regeneration in zebrafish, Hepatology 73 (2021) 1494–1508, https://doi.org/10.1002/hep.31437.
[40] K. Jung, M. Kim, J. So, S.H. Lee, S. Ko, D. Shin, Farnesoid X receptor activation impairs liver progenitor cell-mediated liver regeneration via the PTEN-PI3K-AKT-mTOR Axis in zebrafish, Hepatology (2020), https://doi.org/10.1002/hep.31679.
[41] L. Lebedeva, B. Zhumabayeva, T. Gebauer, I. Kisselev, Z. Aitasheva, Zebrafish (Danio rerio) as a model for understanding the process of caudal fin regeneration, Zebrafish 17 (2020) 359–372, https://doi.org/10.1089/zeb.2020.1926.
[42] Z. Cao, Y. Meng, F. Gong, Z. Xu, F. Liu, M. Fang, L. Zou, X. Liao, X. Wang, L. Luo, X. Li, H. Lu, Calcineurin controls proximodistal blastema polarity in zebrafish fin regeneration, Proc Natl Acad Sci U S A 118 (2021), https://doi.org/10.1073/pnas.2009539118.
[43] C. Pfefferli, A. Jazwinska, The careg element reveals a common regulation of regeneration in the zebrafish myocardium and fin, Nat Commun 8 (2017) 15151, https://doi.org/10.1038/ncomms15151.
[44] C. Pfefferli, A. Jazwinska, The art of fin regeneration in zebrafish, Regeneration (Oxf) 2 (2015) 72–83, https://doi.org/10.1002/reg2.33.
[45] M.L. Kang, J.E. Kim, G.I. Im, Vascular endothelial growth factor -transfected adipose-derived stromal cells enhance bone regeneration and neovascularization from bone marrow stromal cells: Co-transplantation of engineered ADSCs and BMSCs, Journal of Tissue Engineering & Regenerative Medicine 11 (2017). https://onlinelibrary.wiley.com/doi/full/10.1002/term.2247.
[46] Arved Raban, Julian Heller, Tobias Seelig, Patrick Bock, Paul Haubruck, Relation of selenium status to neuro-regeneration after traumatic spinal cord injury, Journal of trace elements in medicine and biology : organ of the Society for Minerals and Trace Elements (GMS) 51 (2018) 141–149, https://doi.org/10.1016/j.jtemb.2018.10.006.
[47] S. Schaefer-Ramadan, C. Thorpe, S. Rozovsky, Site-specific insertion of selenium into the redox-active disulfide of the flavoprotein augmenter of liver regeneration, Archives of Biochemistry & Biophysics 548 (2014) 60–65, https://doi.org/10.1016/j.abb.2014.02.001.
[48] M. Yadid, R. Feiner, T. Dvir, Gold nanoparticle-integrated scaffolds for tissue engineering and regenerative medicine, Nano Letters 19 (2019) 2198–2206, https://doi.org/10.1021/acs.nanolett.9b00472.
[49] P. Nezhad-Mokhtari, M. Akrami-Hasan-Kohal, M. Ghorbani, An injectable chitosan-based hydrogel scaffold containing gold nanoparticles for tissue engineering applications, International Journal of Biological Macromolecules 154 (2020) 198–205, https://doi.org/10.1016/j.ijbiomac.2020.03.112.
[50] L. Wang, S. Li, J. Yin, J. Yang, X. Jiang, The density of surface coating can contribute to different antibacterial activities of gold nanoparticles, Nano Letters 20 (2020) 5036–5042, https://doi.org/10.1021/acs.nanolett.0c01196.
[51] C.M. Chan, C.Y. Hsiao, H.J. Li, J.Y. Fang, D.C. Chang, C.F. Hung, The inhibitory effects of gold nanoparticles on VEGF-A-induced cell migration in choroid-retina endothelial cells, International Journal of Molecular Sciences 21 (2019) 109, https://doi.org/10.3390/ijms21010109.
[52] M. Suleiman, M. Al-Masri, A.A. Ali, D. Aref, I. Warad, Synthesis of nano-sized sulfur nanoparticles and their antibacterial activities, Journal of Materials & Environmental Science 6 (2015) 513–518.
[53] B. Pfxa, B. Zhl, B. Yhd, S.A. Qian, W. Dan, B. Xfza, B. Jxwa, Microfluidic controllable synthesis of monodispersed sulfur nanoparticles with enhanced

antibacterial activities, Chemical Engineering Journal 125293 (2020), https://doi.org/10.1016/j.cej.2020.125293.
[54] S. Shankar, R. Pangeni, W.P. Jin, J.W. Rhim, Preparation of sulfur nanoparticles and their antibacterial activity and cytotoxic effect, Materials Science and Engineering C 92 (2018) 508–517, https://doi.org/10.1016/j.msec.2018.07.015.
[55] H. Forootanfar, M. Adelisardou, M. Nikkhoo, M. Mehrabani, B. Amirheidari, A. R. Shahverdi, M. Shakibaie, Antioxidant and cytotoxic effect of biologically synthesized selenium nanoparticles in comparison to selenium dioxide, Journal of Trace Elements in Medicine & Biology Organ of the Society for Minerals & Trace Elements 28 (2014) 75–79, https://doi.org/10.1016/j.jtemb.2013.07.005.
[56] S.K. Torres, V.L. Campos, C.G. León, et al., Biosynthesis of selenium nanoparticles by Pantoea agglomerans and their antioxidant activity, J Nanopart Res 14 (2012) 1236, https://doi.org/10.1007/s11051-012-1236-3.
[57] H.J. Liu, Y. Qin, Z.H. Zhao, Y. Zhang, T. Sun, Lentinan-functionalized selenium nanoparticles target tumor cell mitochondria via TLR4/TRAF3/MFN1 pathway, Theranostics 10 (2020) 9083–9099, https://doi.org/10.7150/thno.46467.
[58] B. Xla, C. Lwb, C. Jzb, B. Lh, C. Lc, C. Ygb, D. Ccc, E. Yf, L.B. Bai, C. Yflb, Nanosafety evaluation through feces: a comparison between selenium nanoparticles and selenite in rats, Nano Today 36 (2021) 101010, https://doi.org/10.1016/j.nantod.2020.101010.
[59] M. Majidinia, J. Aghazadeh, R. Jahanban-Esfahlani, B. Yousefi, The roles of Wnt/β-catenin pathway in tissue development and regenerative medicine, Journal of Cellular Physiology 233 (2018) 5598–5612, https://doi.org/10.1002/jcp.26265.
[60] Q.M. Nunes, Y. Li, C. Sun, T.K. Kinnunen, D.G. Fernig, Fibroblast growth factors as tissue repair and regeneration therapeutics, PeerJ 4 (2015) e1535, https://doi.org/10.7717/peerj.1535.
[61] C.F. Hsu, H.S. Huang, P.C. Chen, D.C. Ding, T.Y. Chu, IGF-axis confers transformation and regeneration of fallopian tube fimbria epithelium upon ovulation, EBioMedicine (2019) 597–609, https://doi.org/10.1016/j.ebiom.2019.01.061.
[62] W. Reddien, Bermange Peter, L. Adam, M. Kicza, Alvarado Adrienne, A. Sánchez, BMP signaling regulates the dorsal planarian midline and is needed for asymmetric regeneration, Development 134 (2007) 4043–4051, https://doi.org/10.1242/dev.007138.
[63] T.M. Ballhause, S. Jiang, A. Baranowsky, S. Brandt, J. Keller, Relevance of Notch signaling for bone metabolism and regeneration, International Journal of Molecular Sciences 22 (2021) 1325, https://doi.org/10.3390/ijms22031325.
[64] W. Yu, A. Yu, F.X. Yu, The Hippo pathway in tissue homeostasis and regeneration, Protn & Cell 8 (2017) 349–359, https://doi.org/10.1007/s13238-017-0371-0.
[65] B. Singh, N. Koyano-Nakagawa, A. Donaldson, C. Weaver, M. Garry, D. Garry, Hedgehog signaling during appendage development and regeneration, Genes 6 (2015) 417–435, https://doi.org/10.3390/genes6020417.
[66] L. Wu, Y. Gu, L. Liu, J. Tang, W. Cui, Hierarchical micro/nanofibrous membranes of sustained releasing VEGF for periosteal regeneration, Biomaterials 227 (2019) 119555, https://doi.org/10.1016/j.biomaterials.2019.119555.
[67] E.M. Tottoli, R. Dorati, I. Genta, E. Chiesa, B. Conti, Skin wound healing process and new emerging technologies for skin wound Care and regeneration, Pharmaceutics 12 (2020) 735, https://doi.org/10.3390/pharmaceutics12080735.
[68] Cooper Stoick, L. Cristi, Gilbert Weidinger, Riehle, J. Kimberly, Charlotte Hubbert, Distinct Wnt signaling pathways have opposing roles in appendage regeneration, Development 134 (2007) 479–489, https://doi.org/10.1242/dev.001123.
[69] Y. Lee, Fgf signaling instructs position-dependent growth rate during zebrafish fin regeneration, Development 132 (2005) 5173–5183, https://doi.org/10.1242/dev.02101.
[70] N. Ferrara, The role of vascular endothelial growth factor in pathological angiogenesis, Breast Cancer Res Treat 36 (1995) 127–137, https://doi.org/10.1007/BF00666035.
[71] C.W. Hicks, G.Q. Zhang, J.K. Canner, N. Mathioudakis, D. Coon, R.L. Sherman, C. J. Abularrage, Outcomes and predictors of wound healing among patients with complex diabetic foot wounds treated with a dermal regeneration template (integra), Plastic and Reconstructive Surgery 146 (2020) 893–902, https://doi.org/10.1097/PRS.0000000000007166.
[72] L.A. Lavery, D.G. Armstrong, S.A. Vela, T.L. Quebedeaux, J.G. Fleischli, Practical criteria for screening patients at high risk for diabetic foot ulceration, Archives of Internal Medicine 158 (1998) 157–162, https://doi.org/10.1001/archinte.158.2.157.
[73] L. Zang, L.A. Maddison, W. Chen, Zebrafish as a model for obesity and diabetes, Frontiers in Cell and Developmental Biology 6 (2018) 91, https://doi.org/10.3389/fcell.2018.00091.
[74] X. Xie, R. Zhong, L. Luo, X. Lin, L. Huang, S. Huang, L. Ni, B. Chen, R. Shen, L. Yan, C. Duan, The infection characteristics and autophagy defect of dermal macrophages in STZ-induced diabetic rats skin wound Staphylococcus aureus infection model, Immunity 72 (2021) 1–11, https://doi.org/10.1002/iid3.492.